



Geophysical Research Letters*



RESEARCH LETTER

10.1029/2024GL109440

Key Points:

- Melt transport at mid-ocean ridge models reproduce observed frozen melt layers in the oceanic lithosphere
- Frozen melt layers are present regardless of model parameters
- Predicted seismic signatures require further mechanisms to be compatible with observations

Supporting Information:

Supporting Information may be found in the online version of this article.

Correspondence to:

S. J. Sim, jssim@eas.gatech.edu

Citation:

Sim, S. J., Yu, T.-Y., & Havlin, C. (2024). Persistent heterogeneities in the oceanic lithosphere due to differential freezing beneath ridges. *Geophysical Research Letters*, *51*, e2024GL109440. https://doi.org/10.1029/2024GL109440

Received 22 MAR 2024 Accepted 29 OCT 2024

Persistent Heterogeneities in the Oceanic Lithosphere Due To Differential Freezing Beneath Ridges

Shi Joyce Sim¹, Ting-Ying Yu^{1,2}, and Chris Havlin³

¹Georgia Institute of Technology, Atlanta, GA, USA, ²Now at Massachusetts Institute of Technology, Boston, MA, USA, ³University of Illinois at Urbana-Champaign, Champaign, IL, USA

Abstract Oceanic lithosphere, which forms two-thirds of Earth's surface, is generated at mid-ocean ridge spreading centers. Yet the internal structure of the lithosphere is not well characterized and often considered to be homogeneous relative to the structure of continental lithosphere. While geophysical observations clearly delineate the crust-mantle boundary and the lithosphere-asthenopshere boundary, other seismic anomalies known as mid-lithosphere discontinuities (MLDs) have been challenging to detect and poorly constrained. Here we present melt transport models applied to the mid-ocean ridge system that indicate MLDs are a widespread fundamental feature of oceanic lithosphere. In our models, some melt generated from decompression melting is frozen back into the lithosphere, forming a layered refertilization pattern. These refertilized layers are due to the stacked horizontal layering pattern of melt pooling beneath the freezing front. If the recrystallized melt is incorporated into the lithosphere as mafic lenses, the predicted seismic velocity is compatible with observations.

Plain Language Summary Using state of the art numerical models of magma transport within Earth's interior at mid-ocean ridges, we found that the layers observed in the oceanic lithosphere are due to the process of melt freezing close to the ridge axis and are likely ubiquitous beneath the ocean floor. We find that the expected seismic signature would match current observations. This supports the idea of a heterogeneous oceanic lithosphere that will eventually be subducted at a convergence margin. Considering both seismic and electromagnetic observations, the models suggest that the mantle is less permeable and therefore likely stronger than previously thought.

1. Introduction

The oceanic lithosphere covers most of the Earth and eventually subducts back into the mantle as part of plate tectonics. The oceanic lithosphere is typically thought of as a homogeneous structure with the Mohorovičić discontinuity separating the crust and the mantle and the Gutenberg discontinuities, that roughly defines the extent of the oceanic lithosphere (Schmerr, 2012). The Gutenberg discontinuity (G discontinuities) is collectively defined as an observed drop in seismic velocity around 35–120 km beneath the ocean and is sometimes interpreted as the lithosphere-asthenosphere boundary (LAB) (Schmerr, 2012). The boundary between the lithosphere and asthenosphere is a subject of vigorous ongoing debate with important implications for plate tectonics (Fischer et al., 2010; Rychert et al., 2020). G discontinuities and other mid-lithosphere seismic discontinuities have been found in central Pacific (Gaherty et al., 1999; Tan & Helmberger, 2007) and have been attributed to partial melt (Tan & Helmberger, 2007), compositional layering (Gaherty et al., 1999), change in water content (Karato, 2012), or seismic anistropy (Hansen et al., 2016). Recently, seismic surveys show mid-lithosphere seismic discontinuities in the oceanic setting that were suggested as being due to melt produced at mid-ocean ridges that have since frozen into the lithosphere and moved away from the ridge (Kennett & Furumura, 2015; Ohira et al., 2017; Qin et al., 2020). These seismic discontinuities in the shallower lithosphere are enigmatic, hard to differentiate and probe because they are small and shallow.

These features in the oceanic lithosphere were likely molten and dynamic at some point in time, particularly at the mid-ocean ridge where it was formed. While seismic observations give us an in-situ snapshot in time, we employ melt transport modeling or two-phase flow numerical models to investigate these features of dynamic origins. Melt transport in the mantle describes the flow of a less viscous darcian melt through a deformable more viscous mantle matrix (Fowler, 1985; McKenzie, 1984; Scott & Stevenson, 1986). This two-phase flow formulation has been used successfully to study melt transport beneath mid-ocean ridges (Keller et al., 2017; Sim, 2022; Sim

© 2024. The Author(s).

This is an open access article under the terms of the Creative Commons

Attribution-NonCommercial-NoDerivs

License, which permits use and distribution in any medium, provided the original work is properly cited, the use is non-commercial and no modifications or adaptations are made.

SIM ET AL. 1 of 11

19448007, 2024, 23, Downk

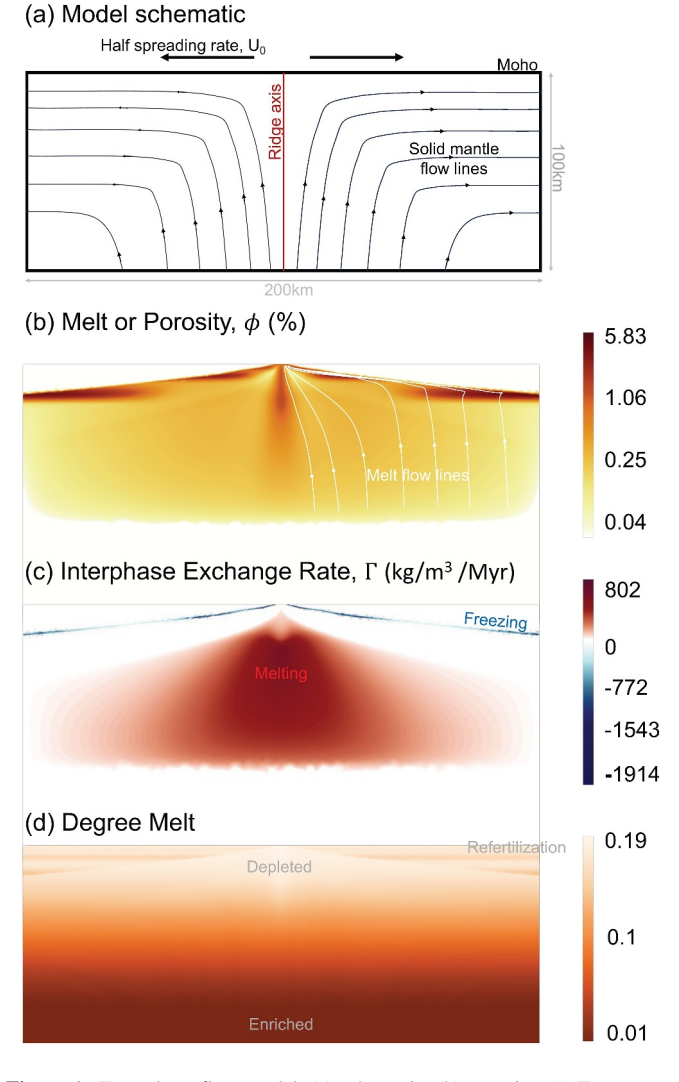


Figure 1. Two-phase flow model: (a) schematic, (b) porosity, (c) Γ (interphase exchange: melting or freezing), and (d) degree melt for model with half spreading, $U_0 = 4$ cm/yr, and background permeability, $K_0 = 4 \times 10^{-7}$ m². For more details, we refer the readers to Sim et al. (2020).

et al., 2020; Turner et al., 2017), subduction zones (Cerpa et al., 2019), mantle plumes (Dannberg & Heister, 2016), shallow carbon storage (Räss et al., 2018) and planetary systems (Spencer et al., 2020). In particular, two-phase flow models of melt transport mid-ocean ridges show that not all the melt escapes to form the oceanic crust but rather some of the melt actually freezes back into the lithosphere during melt transport (Sim et al., 2020; Turner et al., 2017).

2. Two-Phase Flow Models

In this study, we present new analyses along with seismic velocity estimates of six two-dimensional melt migration beneath mic-ocean ridges model outputs from previously published studies (Sim et al., 2020), which varied half spreading rates, $U_0 = 2$, 4, 8 cm/yr and background mantle permeability $K_0 = 4 \times 10^{-7,-9}$ m². To help readers understand the models and the new analyses presented in this work, we briefly describe the models. We show the simple schematic of the model along with a model snapshot for the model output with half spreading rates, $U_0 = 4$ cm/yr and background mantle permeability $K_0 = 4 \times 10^{-7} \text{ m}^2$ (denoted as U4K7) in Figure 1. The model domain is 100 km deep and 200 km wide with the ridge axis at the center. The top boundary is defined by the crust-mantle boundary or the Mohorovic boundary and is prescribed a half spreading rate on either side. The bottom boundary is an upwelling boundary and the side boundaries are outflow boundaries. Melt migration beneath the mid-ocean ridges is modeled using the two-phase flow formulation of Darcy-like fluid flow in a viscously deforming solid mantle following previous works (Fowler, 1985; McKenzie, 1984; Scott & Stevenson, 1984, 1986). Mass, momentum and energy conservation equations are used to solve for solid velocity, dynamic pressure, porosity, compaction pressure and temperature in a one way coupled manner in the limit of small porosities (Sim et al., 2020). Solid shear viscosity is the harmonic sum of diffusion creep, dislocation creep and a small plasticity term. Bulk viscosity is the ratio of solid shear viscosity to porosity. The interphase exchange (melting and freezing) is the exchange of mass between the melt and mantle. The melting parameterization is based on dry peridotite melting (Katz et al., 2003) and depth dependent solidus (Hirschmann, 2000) such that melting is largest beneath the ridge axis where mantle upwelling is the fastest and decreases away from the ridge axis as shown in Figure 1c. The freezing parameterization depends on the temperature difference between the calculated temperature and the liquidus temperature of basalt and is linearly

dependent on the amount of melt present. The freezing front is defined by a thin layer of freezing as shown in Figure 1c. This could be interpreted as the LAB where melt is pooling underneath. Permeability is described by the intrinsic mantle permeability and related exponentially to the porosity. For more details on the numerical models, we refer readers to previous works (Sim, 2022; Sim et al., 2020).

In these melt migration beneath the mid-ocean ridge models, the mantle upwells and melts decompressively beneath the ridge axis as the oceanic plates are spreading apart with imposed velocity on the top boundary. Most of the melt escapes into a narrow region to form the oceanic crust while some of it freezes back into the lithosphere. In the models, roughly 70%–85% of the total melt produced is extracted to make up about 6–7 km of oceanic crust while the rest of the melt (about 15%–30%) eventually refreezes and refertilizes the oceanic lithosphere (Sim et al., 2020). This is similar to the estimated 20%–40% of melt that does not get extracted based on purely melting models that has no freezing (Behn & Grove, 2015). For the suite of model analyses presented in this study, the depths over which freezing occurs (or the thickness of the lithosphere) deepens with decreasing spreading rates as expected, since the plate is older and thicker 100 km away from the ridge axis for a slower spreading case than for a faster spreading case.

SIM ET AL. 2 of 11

3. Enriched Layers in the Oceanic Lithosphere

In this work, we made new analyses of the degree melt in these previously published model outputs and show that these models create refertilized layers in the lithosphere. In these models, the degree melt is defined and tracked as the amount of melting and freezing a parcel of the mantle has experienced as it upwells beneath the mid-ocean ridge and turns the corner, dragged by plate spreading. Therefore, the degree melt is not the same as melt/porosity as shown in Figure 1. The degree melt increases as the parcel of mantle experiences melting and becomes more depleted. On the other hand, the degree melt decreases as melt freezes back into the parcel of mantle, that is, the mantle becomes refertilized and enriched. Degree melt has a mostly one dimensional structure that decreases with depth since it is mainly due to depth-dependent melting and the mantle corner flow beneath mid-ocean ridges (Figure 1c). Since there is no freezing on the ridge axis, the one-dimensional depth profile of degree melt on the ridge axis would be the expected profile everywhere in the two-dimensional model domain if there were no freezing at all. In fact, the initial conditions for degree melt is exactly this one-dimensional profile of degree melt across the two-dimensional model. This is mainly due to melting that is dependent on the mantle upwelling rates and mantle corner flow beneath mid-ocean ridges, such that the melting rate is the largest with the fastest mantle upwelling on the ridge axis (hence largest degree melt at shallow depths) and decreases away from the ridge axis (hence smaller degree melt at deeper depths). The two-dimensional features only shows up in the shallower parts of the model domain where there is freezing. If there were uniform constant freezing along the freezing boundary, degree melt would deviate away from the one-dimensional structure in a uniform manner. However, as shown in the snapshot of the model output for U4K7 in Figure 1c, freezing is not uniform along the freezing boundary in the models and because of this differential freezing and hence refertilization in the models, degree melt forms a horizontally layered structure in the oceanic lithosphere, much like layered sills as shown in Figure 1d. Where there is less freezing, the degree melt for a parcel of mantle remains close to the no freezing profile on the ridge axis and remains depleted. Conversely, where there is more freezing, the degree melt for a parcel of mantle becomes more depressed and the mantle is more refertilized. We note that the degree melt patterns at shallower depths above the freezing zone are completely solid.

Analyses of the depth profile of degree melt (taken at the side boundary of the model outputs, 100 km from the ridge axis) show that the relatively enriched or refertilized layers are typically a few kilometers thick and also a few kilometers apart (Figure 2). The degree melt is detrended by the expected one-dimensional vertical depth profile of degree melt without freezing on the ridge axis such that negative degree melt represents refertilization. The layers are smooth and similar for the models with the same permeability, apart from the slow spreading case. Only the slow spreading and smaller permeability model output (U2K9) has no clear layers but there are still significant refertilization. The layering is particularly distinct for models with less permeable mantle, that is, $k_0 = 4 \times 10^{-9}$ m², with the first layer about a few kilometers deep followed by the next layer a few kilometers down (Figure 2). For models with more permeable mantle, that is, $k_0 = 4 \times 10^{-7}$ m², the deviation of degree melt is of similar magnitude across spreading rates (Figure 2).

Porosity waves are inherent to the physics of two-phase flow models and tend to dissipate with time (Spiegelman, 1993a). They can persist throughout the model time when the model parameters for melt migration beneath mid-ocean ridges are above a critical value (Sim, 2022), otherwise, they dissipate. The transient period of the model is a period of model time at the beginning when there are time-dependent wave-like features (melt-rich porosity waves) present in the models in this work. These transient waves have also been shown in other numerical two-phase flow works on the mid-ocean ridge (Katz, 2010; Keller et al., 2017). The U2K7 model is the only model in this suite of models that has persistent porosity waves beyond the initial transient period. The U2K7 model also has refertilized layering in the lithosphere.

The degree melt or refertilization vertical depth profiles are correlated with the freezing rate and amount of melt (Figure 3). We show the collocated vertical profile degree melt, freezing rate and amount of melt along the freezing front (as shown in Figure 1c) in Figure 3. Ultimately, the refertilization layering pattern is due to the melt organization along the freezing front. The porosity or melt organizes itself into a horizontally layered pattern with varying amounts along the freezing front. This pattern is manifested by dispersive solitary waves fixed in place by the freezing front as described in previous work (Spiegelman, 1993b). The spatial scales of these organized melt layers are governed by the compaction and freezing length scales, both of which change depending on both spreading rates and permeabilities. The degree melt deviation is more significant for models with less permeable background mantle (as shown in Figure 2) precisely because of the larger amount of melt present compared with

SIM ET AL. 3 of 11

19448007, 2024, 23, Downk

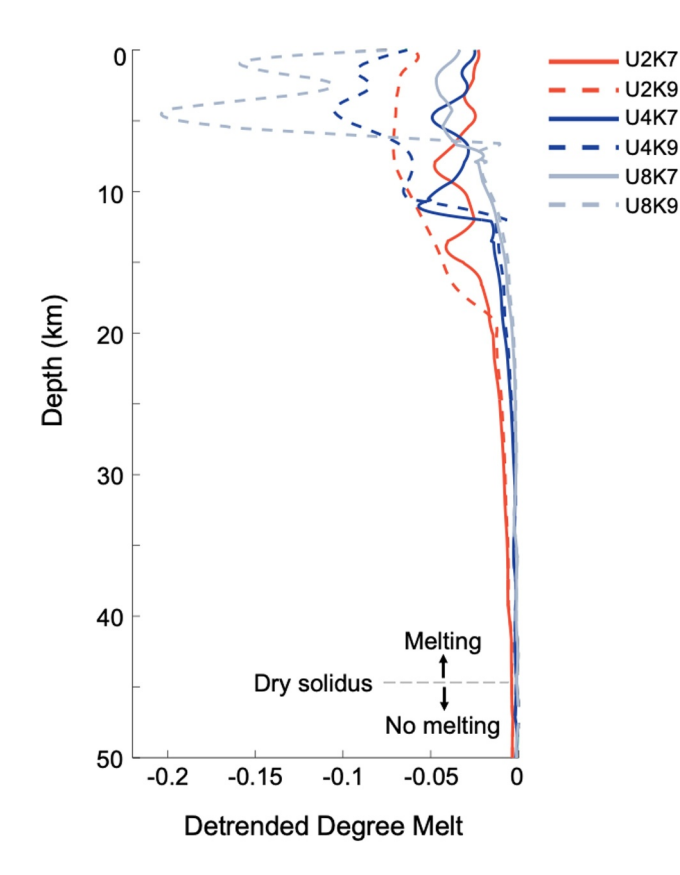


Figure 2. Layers in degree melt profiles: Vertical profile of detrended degree melt at 100 km away from the ridge axis or the side boundary for the suite of models with varying half spreading rates (corresponding colors) and background permeabilities (corresponding line styles). The degree melt is negative due to the detrending as described in the main text. The corresponding age of the oceanic lithosphere is 5, 2.5, 1.25 Myr for plate spreading of 2, 4, 8 cm/yr respectively at 100 km away from the ridge axis. *X*-axis is the detrended degree melt and *y*-axis is the depth.

models with smaller amount of melt present in models with a more permeable mantle (Figure 3). This is because melt transport is relatively sluggish for models with a less permeable mantle and melt sticks around long enough to be frozen into the lithosphere. On the other hand, melt transport is more efficient for models with a more permeable mantle and does not stick around to be frozen, that is, there is less melt. This difference is seen not only in the amount of melt in the model outputs themselves but also in the larger proportion of melt that was not extracted and refroze into the oceanic lithosphere for the less permeable models (Sim et al., 2020).

4. Seismic Signature of Lithospheric Structures in Two-Phase Models

The seismic properties of two-phase model output were calculated for 3 different cases. The first case calculates seismic velocities for an isotropic, olivine-only baseline throughout the model domain. The second case uses the degree of re-fertilization within the lithosphere to represent a volume fraction of a recrystallized, separate basalt-like phase within the lithosphere and calculates an aggregate isotropic velocity using a Voigt average of isotropic endmembers. Finally, the third case accounts for anisotropy within the lithosphere by treating the recrystallized phase as aligned inclusions following (Kendall, 2000; Tandon & Weng, 1984). A fully reproducible set of Python and MATLAB routines is provided in the supplemental materials along with an archive of the data required to reproduce the post-processing (Sim et al., 2023).

For calculating the properties of isotropic endmembers, the Very Broadband Rheology calculator (VBRc, Havlin et al., 2021) was used directly to calculate seismic properties using model outputs. To do so, the temperature, melt fraction and pressure were taken directly from model outputs and interpolated from unstructured mesh to a uniform grid using published python package for interpolation, yt (Havlin, 2023a; Turk et al., 2010). Additionally, anelastic calculations assume a grain size (set to 1 cm), deviatoric stress of 0.1 MPa and a 5 km basaltic crust across the model top. Results are shown for frequency 0.01 Hz (note that the frequency dependence here arises purely

from the frequency dependence of intrinsic attenuation) and the extended-Burgers model (Jackson & Faul, 2010) with unrelaxed moduli and anharmonic derivatives from (Isaak, 1992) accounting for the poro-elastic effect from (Takei, 2002). Additional results are shown for a wider frequency range of 0.001–1 Hz in the online supplement.

For the case in which the degree of melting in the lithosphere is treated as a separate basalt-like phase, the endmember isotropic velocities were calculated as stated above using the VBRc by varying the reference moduli and anharmonic derivatives using basalt-like values for the recrystallized phase (unrelaxed, reference shear modulus of 50 GPa with poisson ratio of 0.25). The volume fraction of the recrystallized phase was calculated as the horizontal difference in degree of melting across the freezing boundary. For the isotropic case, a Voigt average was used to calculate aggregate properties between the mantle- and crust-like phases. For the anisotropic case, the published function pyVBRc (Havlin, 2023b) was used to calculate the effect of aligned inclusions following (Kendall, 2000; Tandon & Weng, 1984) for an aspect ratio of 0.01, corresponding to lenses of melt frozen into the lithosphere. Finally, it is important to note that in referring to a basalt-like phase, we are referring to a seismically slow, secondary phase resulting from recrystallization. The actual composition could range from basalt to more ultramafic composition depending on degree of melt of the source rock and interaction with residual mantle during emplacement and could be further complicated by the presence of volatiles (and possible hydrous phases). Specifically, the presence of volatiles would lead to precipitation of hydrous mineral phases, since the shallow lithosphere will be in the amphibole stability zone (Selway et al., 2015). Hydrous mineral phases can decrease seismic velocities although it is unclear if the melt transport models will yield enough to match observations (Selway et al., 2015). This would also require including volatile transport in the models (Keller et al., 2017) which is motivation for future work.

SIM ET AL. 4 of 11

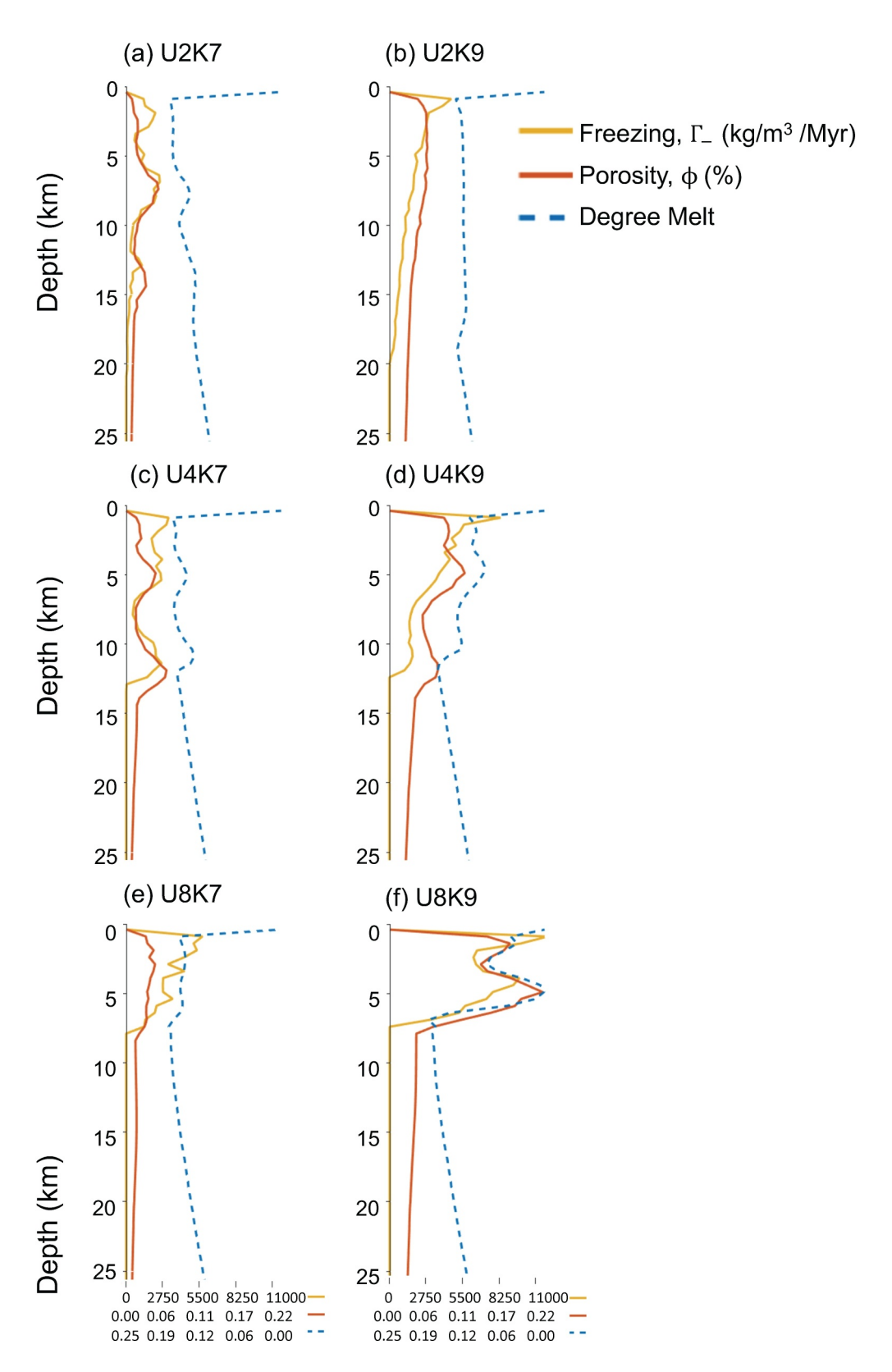


Figure 3. Correlation of porosity, freezing rate and degree melt: Vertical depth profile of maximum freezing rate, Γ_- , corresponding porosity, ϕ , and degree melt all taken at depths corresponding to the freezing front for the suite of models with varying half spreading rates, $U_0 = 2$, 4, 8 cm/yr and background permeabilities, $K_0 = 4 \times 10^{-7}$, 9m². Such that (a-b) $U_0 = 2$ cm/yr, (c-d) have $U_0 = 4$ cm/yr and (e-f) $U_0 = 8$ cm/yr and plots on the left column correspond to models with larger permeabilities, $K_0 = 4 \times 10^{-7}$ m², while the plots on the right column correspond to models with smaller permeabilities, $K_0 = 4 \times 10^{-9}$ m².

SIM ET AL. 5 of 11

19448007, 2024, 23, Downloaded from https://agupubs.

onlinelibrary.wiley.com/doi/10.1029/2024GL109440 by Readcube (Labtiva Inc.), Wiley Online Library on [18/12/2024]

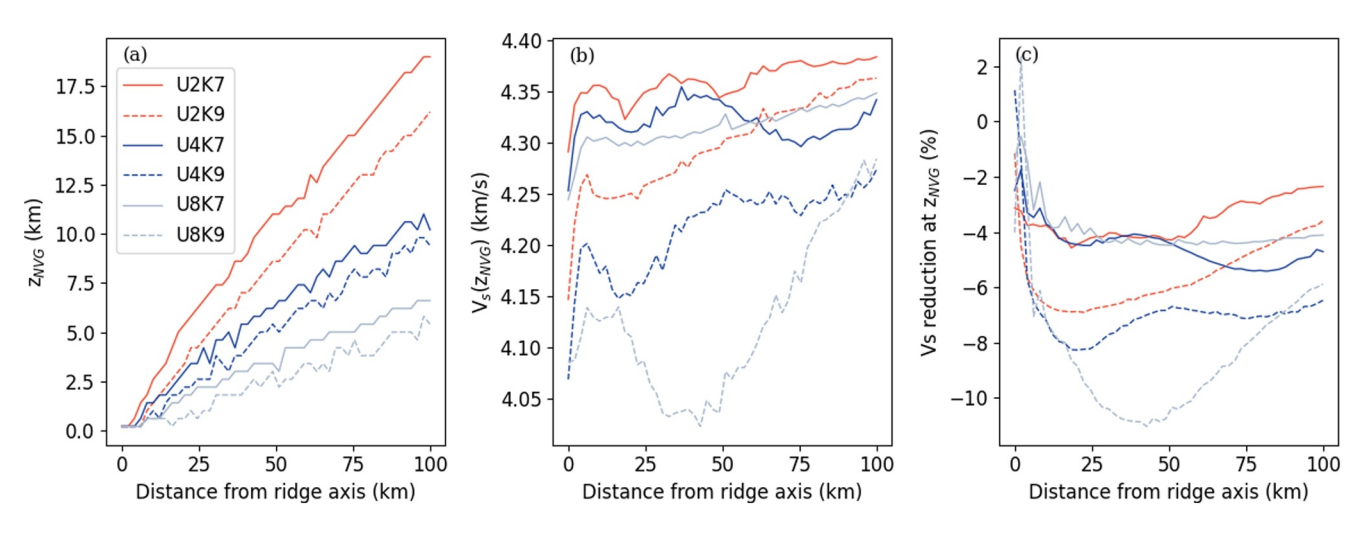


Figure 4. Seismic estimates for negative velocity gradient (NVG) coincident with the freezing interface as discussed in the text: Predicted NVG seismic characteristics versus distance from the ridge: (a) depth to the seismic NVG, z_{NVG} , (b) shear wave speed at the NVG, $V_s(z_{NVG})$, and (c) percent reduction in V_s at the NVG.

The analyses of the two-phase flow models presented here predict a number of interesting spatial variations in the seismic signature of both the LAB and the internal seismic structure of the oceanic lithosphere. Because the rheologically defined LAB may not coincide with seismically imaged boundaries, we use the negative velocity gradient (NVG) coincident with the freezing interface within the models where there is a decrease in shear wave velocity with increasing depth. The seismic characteristics of the NVG in the two-phase models are calculated directly from model output. Figure 4 shows the NVG depth, seismic shear wave velocity, V_s , and the drop in V_s at the NVG as a function of distance from the ridge axis for all two-phase flow models for the first case described in the methods.

While the depth to the NVG increases with age, similar to a standard conductive thermal boundary layer (half-space cooling), the shear wave velocity at the NVG varies significantly with distance from the ridge due to the porosity structure with strong velocity reductions where melt pools. Additionally, the reduction in V_s (the strength of the NVG) is primarily controlled here by the varying melt fraction, resulting in a reduction that occurs over less than a few km. Because the minimum V_s occurs within a narrow boundary layer where melt accumulates, we compute the V_s reduction by comparing average values within ± 10 km of the freezing interface.

Calculating the seismic signature of the oceanic lithosphere from the two-phase flow model outputs depends critically on the recrystallization of melt across the freezing boundary. If recrystallization occurs as an equilibrium process resulting simply in refertilization of the mantle, the seismic effect will be negligible (Schutt & Lesher, 2006). If, however, crystallization occurs in a more dynamic fashion, resulting in a secondary basalt-like phase, then the effect on seismic properties will be stronger. Where melt accumulates at the freezing interface, it is possible that the assumption of purely viscous deformation in the two-phase flow models breaks down, resulting in more rapid transport of melt in dikes or sills (Havlin et al., 2013). By treating the change in refertilization fraction across the LAB as a volume fraction of a recrystallized, secondary basalt-like phase, we can place limits on the seismic characteristics of the frozen melt within the lithosphere predicted by the two-phase model. For the isotropic case as shown in Figure 5a, the variations in compressional wavespeed, V_p , within the lithosphere remain relatively small. If the crystallization results in intrinsic anisotropic fabrics, the larger spreading rates exhibit 1-2% maximum intrinsic anisotropy in V_p . The predicted anisotropy from the basalt inclusions is too small to explain anisotropy observations from active source (Hess, 1964; Kodaira et al., 2014)) and the compositional layering is also likely to be small to explain the observed velocity decreases with depth from scattered waves (Rychert & Harmon, 2017). To estimate the observed anisotropy, we would need to do full waveform study which is beyond the scope of this work but motivates future work. Finally, if further dynamic melt segregation were to concentrate melt into sills of pure melt, then the velocity drop would be similar to observations requiring around a 7% drop in V_p (Ohira et al., 2017). In the present models, a single aggregate layer ranges in thickness from around 100-700 m between models, but based on the model outputs, this recrystallized pure MORB melt would be accumulating in a few layers.

SIM ET AL. 6 of 11

19448007, 2024, 23, Downloaded from https://agupubs.onlinelibrary.wiley.com/doi/10.1029/2024GL109440 by Readcube (Labtiva Inc.), Wiley Online Library on [18/12/2024]. See the Terms

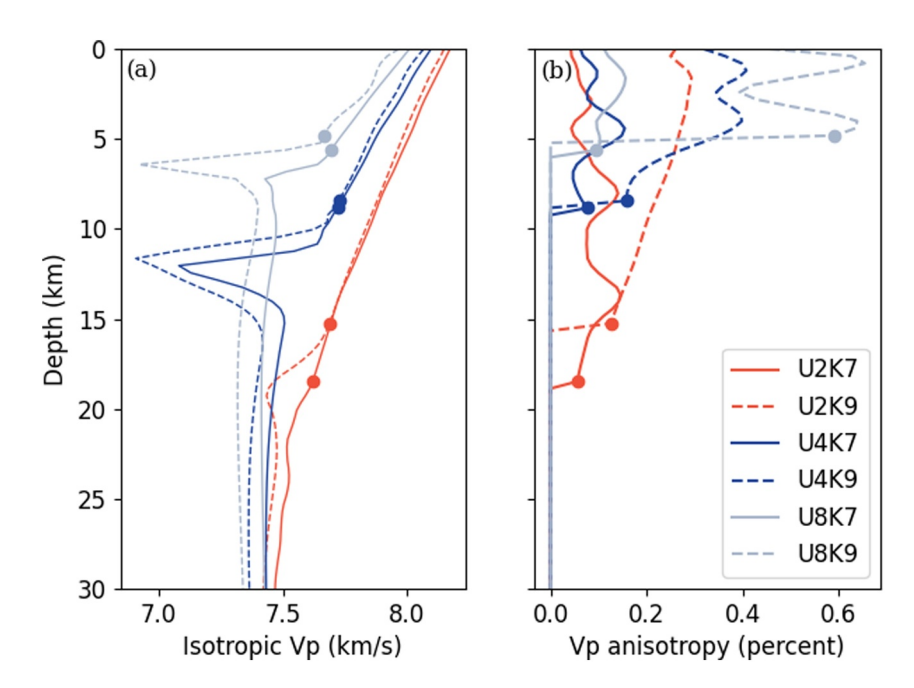


Figure 5. Seismic estimates from models: Predicted compressional velocity characteristics 100 km away from the ridge axis (see Figure 2 for lithosphere ages) that includes a separate basalt-like phase refrozen in the lithosphere. (a) Isotropic V_p and (b) percent anisotropy for refrozen melts that crystallize in melt lenses within the lithosphere above an isotropic asthenosphere. Circles indicate the depth of the freezing front, below which (at greater depths) the material is partially molten.

5. A Heterogeneous Oceanic Lithosphere

This enrichment fabric is persistent regardless of spreading rate or permeability or porosity waves, suggesting that these horizontal frozen melt layers that vary in the vertical sense may be widespread and ubiquitous in the oceanic lithosphere. This is not surprising given the melt organization predicted by the melt migration models and the correlation of the amount of melt, freezing rates and refertilization, but this had never been demonstrated until this study. Previous melt migration models are expected to produce such refertilized layers as well, given the organization of the melt in the models (Keller et al., 2017; Turner et al., 2017). For example, melt migration models that took into account volatiles transport showed blobs of melt-rich region that would have created variations in refertilization in the lithosphere as well (Keller et al., 2017). Furthermore, another melt migration model taking into account grain size migration also had varying amounts of melt along the freezing front (Turner et al., 2017). Given that a simple model of melt migration suggests that these refertilized features in the lithosphere are persistent, it is no doubt that adding more complexities such as mantle heterogeneities to the models will strengthen this hypothesis of a heterogeneous lithosphere created due to melt migration processes beneath the mid-ocean ridge. In fact, melt migration models with mantle heterogeneities do show blobs of melt-rich regions that will promote the persistence of this feature (Weatherley & Katz, 2016).

There are many seismic observations of layers in the lithosphere, including those inferred to delineate the lithosphere from the asthenosphere, but their origins are hard to constrain (Gaherty et al., 1999; Kennett & Furumura, 2015; Ohira et al., 2017; Qin et al., 2020; Tan & Helmberger, 2007; Tharimena et al., 2017). We compare the vertical depth profiles of the refertilized layers from our models with recent observed seismic layers from both slow and fast spreading ridges (Gaherty et al., 1999; Kennett & Furumura, 2015; Ohira et al., 2017; Qin et al., 2020). As shown in Figure 5, the basalt inclusions are decreases velocities at shallow depths and melt at the base of the permeability boundary are responsible for the large velocity drop at the NVG. On the slower spreading young Juan de Fuca plate, the two sub-horizontal reflections at 11 and 14.5 km below seafloor that are about 300–600 m thick with observed seismic velocity drop 7%–8% in V_p (Qin et al., 2020) can be reproduced by refertilized layers in the model with larger permeability (U2K7) with regards to the length scale and distance apart of the layers. As discussed in the previous section, the layers predicted by the models would have to be a sill of pure frozen melt in order to reproduce the observed seismic velocity drop of 7%–8% in V_p . On the older and faster spreading Pacific plate (148-128 Ma), seismic evidence suggests the presence of 2 km thick lenses with gradual

SIM ET AL. 7 of 11

velocity decrease of 7% around 35–60 km depths in V_p (Ohira et al., 2017). It is unclear whether there are any similar features shallower than 35 km on the Pacific plate due to the limitations of the survey (Ohira et al., 2017). For the two-phase flow models with comparable fast spreading rates observed for the older Pacific plate (U8K7 and U8K9), there are shallow refertilized layers a few kilometers thick and a few kilometers apart, but there are no enriched layers deeper than 10 km below the Moho. As shown here, our models are compatible with seismic observations at one place but perhaps raise further questions at another. This highlights the limitations of both the observations and models that motivate future work.

These mid-lithosphere seismic features have been hypothesized to be due to (a) melt frozen into the lithosphere near the ridge axis (Kennett & Furumura, 2015; Ohira et al., 2017; Qin et al., 2020), (b) shallow partially molten sills (Oin et al., 2020) and/or, lastly (c) melt percolating upwards from a deeper source away from the ridge axis (Tharimena et al., 2017). Being able to differentiate between these scenarios has implications for post-seismic deformation at the subduction zone (Agata et al., 2019; Freed et al., 2017). Our model results suggest that these seismic features are likely due to melt frozen into the lithosphere as a consequence of melt migration processes beneath mid-ocean ridges as opposed to the other two hypotheses. We emphasize that even though the processes are aligned, for the subsolidus/lithospheric portion of the model and at the volume fractions of recrystallized melt (the basalt-like phase) predicted by the model, it is hard to have a strong signal in isotropic or anisotropic variations and the seismic post-processing of the model outputs cannot reproduce the magnitude of seismic observations without additional processes that we do not model. To obtain a stronger signal like those observed: (a) larger volume fractions of frozen-in melt (presumably via melt focusing/intrusion mechanisms not included in the model) or (b) thermodynamically stable partially molten layering (in line with the second hypothesis). In support of the second hypothesis, it is possible that these melts were not frozen into the lithosphere right away close to the ridge axis but were trapped in the oceanic lithosphere as it advected away from the ridge axis. However, melt is not stable in the oceanic lithosphere even with an enriched mantle with large amounts of volatiles (Hirschmann, 2010). The trapped melt could potentially stay molten for an extended period of time as it becomes increasingly enriched (therefore harder and harder to freeze) as it slowly freezes away into the surrounding lithosphere as evidenced by long-lived melt channels beneath the LAB (Naif et al., 2013). The long-lived melt channels off the coast of central America might be plume related (Naif et al., 2023) and therefore presents a unique case that supports the third hypothesis. This motivates further in-depth studies using more robust thermodynamics parameterization to better understand the resulting petrology from this freezing process beneath the mid-ocean ridge.

Considering electromagnetic together with the seismic observations, the steep LAB as suggested by an electromagnetic survey at the East Pacific Rise (Key et al., 2013) would also agree with the hypothesized thicker lithosphere with frozen melt sills (hypothesis 1 in previous paragraph). This steep LAB is contrary to most melt transport models, which dictates a shallow gently sloped LAB. Previous melt migration models that could explain this steep LAB imposed a steep freezing front so it was hard to discern if this was indeed the result of the modeled physics or an artifact of the imposed freezing front (Turner et al., 2017). From the melt transport modeling perspective, there are two ways to reconcile this discrepancy: (a) the mantle is stronger than is thought since this would result in stronger melt focusing as shown in previous work (Sim et al., 2020) and/or (b) the heat flow near the mid-ocean ridge is underestimated in the models and we need to take into account hydrothermal circulation in the models which would likely result in a steeper thermal profile. Stronger melt focusing means that any melt generated beneath the ridge is pulled strongly toward the ridge axis before it can buoyantly rise to shallower depths away from the ridge, thus forming a steeper LAB that is detectable by electromagnetic methods. Previous models that have stronger melt focusing had to invoke a stronger mantle (Sim et al., 2020).

The model analyses presented in this work have their limitations since (a) they do not have enriched or refertilized layers that extend deeper simply because of the model domain size, (b) the freezing parameterization is simple such that does not take into account changing petrology during the freezing process and (c) the models do not consider how magmatic waves change the melt organization over time and hence the refertilized layers. Since dry peridotite melting begins at 60 km, refertilized layers up to such depths are expected. Furthermore, if we take into account wet melting, the melting depths will increase up to 100–150 km for hydrous or carbonitite melts, therefore potentially increasing the depths of these enriched layers although hydrous melting will not add much more melt (Katz et al., 2003; Keller et al., 2017). These two-phase flow models also do not take into account the fact that trapped melt becomes increasingly enriched as it freezes as discussed above. Moreover, freezing trapped melt with volatiles becomes increasingly hard as

SIM ET AL. 8 of 11

19448007, 2024, 23, Downloa

Acknowledgments

We thank Ben Holtzman, Jessica Warren

and Samer Naif for helpful discussions.

We appreciate two anonymous reviewers

for helpful comments and suggestions

that greatly improved this manuscript.

This research was supported in part

through research cyberinfrastructure

Environment (PACE) at the Georgia

USA. T.Y.Y. was supported by the

President's Undergraduate Research

material is based in part upon work

supported by the National Science

Foundation under Grant 2217616.

Award at the Georgia Institute of

resources and services provided by the

Partnership for an Advanced Computing

Institute of Technology, Atlanta, Georgia,

Technology, Atlanta, Georgia, USA. This

the volatiles become increasingly concentrated as it stays in the melt, thus changing the liquidus. Taken together, this likely means that our analyses of these two-phase flow model outputs give us the minimum degree of melting or enrichment/refertilization expected. The deeper lenses were also observed on Pacific plate that is fairly old, which means that the oceanic plate has since subsided and accumulated kilometers of sediments on top. The two-phase flow models also do not crystallize a pure sill of basaltic melt but rather incorporate the melt back into the residual mantle lithosphere. Crystallizing a pure sill of Wehrlite in a typical residual harzburgite mantle will no doubt make the estimated velocity drop larger from the two-phase flow model outputs and therefore comparable to the observations (Hacker et al., 2003; Ohira et al., 2017). Melt-rich porosity waves beneath mid-ocean ridges can persist in these melt migration models and also result in refertilized layers as shown by the U2K7 model. As discussed in the previous section, these magmatic waves are an inherent time-dependent feature of the physics of two-phase flow numerical models, but it is unclear how these persistent magmatic waves actually affect the refertilized features.

In conclusion, analyses of the refertilization and seismic estimates of two-phase flow models suggest that melt frozen into the oceanic lithosphere is ubiquitous and widespread regardless of spreading rates, permeability and the presence or absence of porosity waves. The model analyses show smooth refertilized horizontal layers in the lithosphere of certain thicknesses, that is correlated with freezing and melt organization. The seismic velocities estimated from the melt migration models are modest compared to current observations but adding complexity will amplify this since these model outputs predict the minimum refertilization. This flips the idea of a homogeneous oceanic lithosphere and requires rethinking about how this heterogeneous oceanic lithosphere subducts. Crucially, it will be important to consider the implications when this heterogeneous oceanic lithosphere subducts. This will hopefully motivate future geophysical surveys to sample the oceanic lithosphere to detect these features and future modeling efforts to better understand the physics and thermodynamics of melt freezing at mid-ocean ridges.

Conflict of Interest

The authors declare no conflicts of interest relevant to this study.

Data Availability Statement

All codes and model outputs are openly available (Sim et al., 2023).

References

Agata, R., Barbot, S. D., Fujita, K., Hyodo, M., Iinuma, T., Nakata, R., et al. (2019). Rapid mantle flow with power-law creep explains deformation after the 2011 Tohoku mega-quake. *Nature Communications*, 10(1), 1385. https://doi.org/10.1038/s41467-019-08984-7

Behn, M. D., & Grove, T. L. (2015). Melting systematics in mid-ocean ridge basalts: Application of a plagioclase-spinel melting model to global variations in major element chemistry and crustal thickness. *Journal of Geophysical Research: Solid Earth*, 120(7), 4863–4886. https://doi.org/10.1002/2015jb011885

Cerpa, N. G., Wada, I., & Wilson, C. R. (2019). Effects of fluid influx, fluid viscosity, and fluid density on fluid migration in the mantle wedge and their implications for hydrous melting. *Geosphere*, 15(1), 1–23. https://doi.org/10.1130/ges01660.1

Dannberg, J., & Heister, T. (2016). Compressible magma/mantle dynamics: 3-d, adaptive simulations in aspect. *Geophysical Journal International*, 207(3), 1343–1366. https://doi.org/10.1093/gji/ggw329

Fischer, K. M., Ford, H. A., Abt, D. L., & Rychert, C. A. (2010). The lithosphere-asthenosphere boundary. *Annual Review of Earth and Planetary Sciences*, 38(1), 551–575. https://doi.org/10.1146/annurev-earth-040809-152438

Fowler, A. (1985). A mathematical model of magma transport in the asthenosphere. *Geophysical & Astrophysical Fluid Dynamics*, 33(1–4), 63–96. https://doi.org/10.1080/03091928508245423

Freed, A. M., Hashima, A., Becker, T. W., Okaya, D. A., Sato, H., & Hatanaka, Y. (2017). Resolving depth-dependent subduction zone viscosity and afterslip from postseismic displacements following the 2011 Tohoku-oki, Japan earthquake. *Earth and Planetary Science Letters*, 459, 279–290. https://doi.org/10.1016/j.epsl.2016.11.040

Gaherty, J. B., Kato, M., & Jordan, T. H. (1999). Seismological structure of the upper mantle: A regional comparison of seismic layering. *Physics of the Earth and Planetary Interiors*, 110(1–2), 21–41. https://doi.org/10.1016/s0031-9201(98)00132-0

Hacker, B. R., Abers, G. A., & Peacock, S. M. (2003). Subduction factory 1. theoretical mineralogy, densities, seismic wave speeds, and H₂O contents. *Journal of Geophysical Research*, 108(B1). https://doi.org/10.1029/2001jb001127

Hansen, L. N., Qi, C., & Warren, J. M. (2016). Olivine anisotropy suggests Gutenberg discontinuity is not the base of the lithosphere. Proceedings of the National Academy of Sciences, 113(38), 10503–10506. https://doi.org/10.1073/pnas.1608269113

Havlin, C. (2023a). data-exp-lab/yt_aspect: Release v0.2.0. Zenodo. https://doi.org/10.5281/zenodo.10150322

Havlin, C. (2023b). vbr-calc/pyvbrc: Release v0.3.1. Zenodo. https://doi.org/10.5281/zenodo.10120446

Havlin, C., Holtzman, B. K., & Hopper, E. (2021). Inference of thermodynamic state in the asthenosphere from an elastic properties, with applications to north American upper mantle. *Physics of the Earth and Planetary Interiors*, 314, 106639. https://doi.org/10.1016/j.pepi.2020. 106639

SIM ET AL. 9 of 11

- Havlin, C., Parmentier, E., & Hirth, G. (2013). Dike propagation driven by melt accumulation at the lithosphere–asthenosphere boundary. *Earth and Planetary Science Letters*, 376, 20–28. https://doi.org/10.1016/j.epsl.2013.06.010
- Hess, H. (1964). Seismic anisotropy of the uppermost mantle under oceans. Nature, 203(4945), 629-631. https://doi.org/10.1038/203629a0
- Hirschmann, M. M. (2000). Mantle solidus: Experimental constraints and the effects of peridotite composition. Geochemistry, Geophysics, Geosystems, 1(10). https://doi.org/10.1029/2000gc000070
- Hirschmann, M. M. (2010). Partial melt in the oceanic low velocity zone. *Physics of the Earth and Planetary Interiors*, 179(1–2), 60–71. https://doi.org/10.1016/j.pepi.2009.12.003
- Isaak, D. G. (1992). High-temperature elasticity of iron-bearing olivines. *Journal of Geophysical Research*, 97(B2), 1871–1885. https://doi.org/10.1029/91jb02675
- Jackson, I., & Faul, U. H. (2010). Grainsize-sensitive viscoelastic relaxation in olivine: Towards a robust laboratory-based model for seismological application. Physics of the Earth and Planetary Interiors, 183(1-2), 151-163. https://doi.org/10.1016/j.pepi.2010.09.005
- Karato, S.-i. (2012). On the origin of the asthenosphere. Earth and Planetary Science Letters, 321, 95–103. https://doi.org/10.1016/j.epsl.2012. 01.001
- Katz, R. F. (2010). Porosity-driven convection and asymmetry beneath mid-ocean ridges. Geochemistry, Geophysics, Geosystems, 11(11). https://doi.org/10.1029/2010gc003282
- Katz, R. F., Spiegelman, M., & Langmuir, C. H. (2003). A new parameterization of hydrous mantle melting. Geochemistry, Geophysics, Geo-
- systems, 4(9). https://doi.org/10.1029/2002gc000433 Keller, T., Katz, R. F., & Hirschmann, M. M. (2017). Earth and planetary science letters. Earth and Planetary Science Letters, 464, 55–68. https://
- doi.org/10.1016/j.epsl.2017.02.006

 Kendall, J.-M. (2000). Seismic anisotropy in the boundary layers of the mantle. In *Geophysical monograph series* (Vol. 117, pp. 133–159).
- American Geophysical Union. https://doi.org/10.1029/gm117p0133

 Kennett, B., & Furumura, T. (2015). Toward the reconciliation of seismological and petrological perspectives on oceanic lithosphere hetero-
- geneity. Geochemistry, Geophysics, Geosystems, 16(9), 3129–3141. https://doi.org/10.1002/2015gc006017
- Key, K., Constable, S., Liu, L., & Pommier, A. (2013). Electrical image of passive mantle upwelling beneath the northern East Pacific Rise. Nature, 495(7442), 499–502. https://doi.org/10.1038/nature11932
- Kodaira, S., Fujie, G., Yamashita, M., Sato, T., Takahashi, T., & Takahashi, N. (2014). Seismological evidence of mantle flow driving plate motions at a palaeo-spreading centre. *Nature Geoscience*, 7(5), 371–375. https://doi.org/10.1038/ngeo2121
- McKenzie, D. (1984). The generation and compaction of partially molten rock. *Journal of Petrology*, 25(3), 1–53. https://doi.org/10.1093/petrology/25.3.713
- Naif, S., Key, K., Constable, S., & Evans, R. (2013). Melt-rich channel observed at the lithosphere–asthenosphere boundary. *Nature*, 495(7441), 356–359. https://doi.org/10.1038/nature.11939
- Naif, S., Miller, N. C., Shillington, D. J., Bécel, A., Lizarralde, D., Bassett, D., & Hemming, S. R. (2023). Episodic intraplate magmatism fed by a long-lived melt channel of distal plume origin. *Science Advances*, 9(23), eadd3761. https://doi.org/10.1126/sciadv.add3761
- Ohira, A., Kodaira, S., Nakamura, Y., Fujie, G., Arai, R., & Miura, S. (2017). Evidence for frozen melts in the mid-lithosphere detected from active-source seismic data. *Scientific Reports*, 7(1), 15770. https://doi.org/10.1038/s41598-017-16047-4
- Qin, Y., Singh, S. C., Grevemeyer, I., Marjanović, M., & Roger Buck, W. (2020). Discovery of flat seismic reflections in the mantle beneath the young Juan de Fuca Plate. *Nature Communications*, 11(1), 4122. https://doi.org/10.1038/s41467-020-17946-3
- Räss, L., Simon, N. S., & Podladchikov, Y. Y. (2018). Spontaneous formation of fluid escape pipes from subsurface reservoirs. *Scientific Reports*, 8(1), 11116. https://doi.org/10.1038/s41598-018-29485-5
- Rychert, C. A., & Harmon, N. (2017). Constraints on the anisotropic contributions to velocity discontinuities at 60 km depth beneath the Pacific. Geochemistry, Geophysics, Geosystems, 18(8), 2855–2871. https://doi.org/10.1002/2017gc006850
- Rychert, C. A., Harmon, N., Constable, S., & Wang, S. (2020). The nature of the lithosphere-asthenosphere boundary. *Journal of Geophysical Research: Solid Earth*, 125(10), e2018JB016463, https://doi.org/10.1029/2018jb016463
- Schmerr, N. (2012). The Gutenberg discontinuity: Melt at the lithosphere-asthenosphere boundary. Science, 335(6075), 1480–1483. https://doi.org/10.1126/science.1215433
- Schutt, D., & Lesher, C. (2006). Effects of melt depletion on the density and seismic velocity of garnet and spinel lherzolite. *Journal of Geophysical Research*, 111(B5). https://doi.org/10.1029/2003jb002950
- Scott, D. R., & Stevenson, D. J. (1984). Magma solitons. Geophysical Research Letters, 11(11), 1161–1164. https://doi.org/10.1029/gl011i011p01161
- Scott, D. R., & Stevenson, D. J. (1986). Magma ascent by porous flow. *Journal of Geophysical Research*, 91(B9), 9283–9296. https://doi.org/10.1029/jb091ib09p09283
- Selway, K., Ford, H., & Kelemen, P. (2015). The seismic mid-lithosphere discontinuity. Earth and Planetary Science Letters, 414, 45–57. https://doi.org/10.1016/j.epsl.2014.12.029
- Sim, S. J. (2022). Persistent magma-rich waves beneath mid-ocean ridges explain long periodicity on ocean floor fabric. *Geophysical Research Letters*, 49(12), e2022GL098110. https://doi.org/10.1029/2022gl098110
- Sim, S. J., Spiegelman, M., Stegman, D. R., & Wilson, C. (2020). The influence of spreading rate and permeability on melt focusing beneath midocean ridges. *Physics of the Earth and Planetary Interiors*, 304, 106486. https://doi.org/10.1016/j.pepi.2020.106486
- Sim, S. J., Yu, T.-Y., & Havlin, C. (2023). Frozen melt data [software]. Zenodo. https://doi.org/10.5281/zenodo.10288494
- Spencer, D. C., Katz, R. F., Hewitt, I. J., May, D. A., & Keszthelyi, L. P. (2020). Compositional layering in Io driven by magmatic segregation and volcanism. *Journal of Geophysical Research: Planets*, 125(9), e2020JE006604. https://doi.org/10.1029/2020je006604
- Spiegelman, M. (1993a). Flow in deformable porous media. Part 1: Simple analysis. *Journal of Fluid Mechanics*, 247(1), 17–38. https://doi.org/10.1017/s0022112093000369
- Spiegelman, M. (1993b). Physics of melt extraction: Theory, implications and applications. *Philosophical Transactions of the Royal Society A: Mathematical, Physical & Engineering Sciences*, 342(1663), 23–41.
- Takei, Y. (2002). Effect of pore geometry on vp/vs: From equilibrium geometry to crack. *Journal of Geophysical Research*, 107(B2), ECV-6. https://doi.org/10.1029/2001jb000522
- Tan, Y., & Helmberger, D. V. (2007). Trans-pacific upper mantle shear velocity structure. Journal of Geophysical Research, 112(B8). https://doi.org/10.1029/2006jb004853
- Tandon, G. P., & Weng, G. J. (1984). The effect of aspect ratio of inclusions on the elastic properties of unidirectionally aligned composites. Polymer Composites, 5(4), 327–333. https://doi.org/10.1002/pc.750050413
- Tharimena, S., Rychert, C., & Harmon, N. (2017). A unified continental thickness from seismology and diamonds suggests a melt-defined plate. Science, 357(6351), 580–583. https://doi.org/10.1126/science.aan0741

SIM ET AL. 10 of 11



Geophysical Research Letters

10.1029/2024GL109440

Turk, M. J., Smith, B. D., Oishi, J. S., Skory, S., Skillman, S. W., Abel, T., & Norman, M. L. (2010). yt: A multi-code analysis toolkit for astrophysical simulation data. *The Astrophysical Journal - Supplement Series*, 192(1), 9. https://doi.org/10.1088/0067-0049/192/1/9

Turner, A. J., Katz, R. F., Behn, M. D., & Keller, T. (2017). Magmatic focusing to mid-ocean ridges: The role of grain-size variability and non-Newtonian viscosity. *Geochemistry, Geophysics, Geosystems*, 18(12), 4342–4355. https://doi.org/10.1002/2017gc007048

Weatherley, S. M., & Katz, R. F. (2016). Melt transport rates in heterogeneous mantle beneath mid-ocean ridges. *Geochimica et Cosmochimica Acta*, 172, 39–54. https://doi.org/10.1016/j.gca.2015.09.029

SIM ET AL. 11 of 11